Journal of Materials Chemistry C

Accepted Manuscript

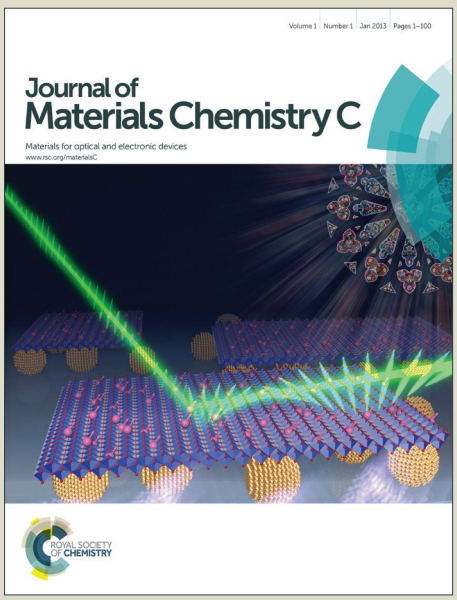

ROYAL SOCIETY OF CHEMISTRY

www.rsc.org/materialsC

Journal Name

ARTICLE

KuQuinones: a new class of quinoid compounds as photoactive species on ITO

Received 00th January 20xx,
Accepted 00th January 20xx

DOI: 10.1039/x0xx00000x

www.rsc.org/

F. Sabuzi, V. Armuzza, V. Conte, B. Floris, M. Venanzi, P. Galloni* and E. Gatto*

KuQuinones constitute a new class of quinoid compounds, characterized by a broad absorption spectrum in the visible region, mainly due to their pentacyclic, highly conjugated structure, and a very low reduction potential. These properties make them promising candidates as sensitive material in photoelectrochemical devices. To this purpose, photocurrent generation measurements have been performed, in presence of an electron donor species in solution, using two different derivatives, 1-(9-hydroxynonyl)KuQuinone ($KuQ(CH_2)_9OH$) and 1-methylKuQuinone ($KuQCH_3$), as photoactive species on indium-tin oxide surface. Electrodes have been functionalized by Langmuir-Blodgett technique, which allowed to easily prepare homogeneous mono- and multilayers of such molecules. Promising results in terms of Incident Photon to Current Efficiency values (IPCE %) and internal quantum efficiency (Φ %) have been achieved. Furthermore, the significance of the organization of the thin film obtained for the efficiency of the electron transfer process has been evidenced.

Introduction

Electron transfer reactions are fundamental processes in many areas of chemistry, physics, and biology. Quinones are a broad class of compounds usually involved in electron transfer reactions, playing key roles in many fundamental biological processes, such as photosynthesis[1] and cellular respiration[2]. In this regard, quinones derivatives are typically present in biologically active molecules; specifically, plastoquinone and phylloquinone are the electron acceptors in photosynthesis[1], while ubiquinone is an essential component in aerobic respiration[2]. Furthermore, many natural and artificial substances, such as dyes and pigments, are quinone derivatives and they can be also used as electroactive materials in redox flow batteries[3] or in photoelectrochemical water oxidation process[4] as well as dyads systems, usually coupled with porphyrins[5], acting as final electron acceptor molecules. Thanks to their ability to take part in electron transfer processes, quinones (Q) have been widely used in electrochemical studies[6]. Their redox behavior is well known: quinones usually undergo two successive one-electron reduction steps to produce firstly semiquinone ($Q^{\bullet-}$) and successively the fully reduced dianion species (Q^{2-}). It is the capability of such molecules to accept one or two electrons that allows them to perform their functions in the electron transport chain and to participate in vital electron transfer processes.

Few years ago, KuQuinones (KuQ), a new class of quinoid compounds, have been synthesized for the first time by a one-pot reaction, starting from reasonably cheap materials[7]. The peculiar characteristic of such compounds is their pentacyclic fully conjugated skeleton, which confers them interesting properties in solution (Scheme 1). They show a broad absorption spectrum in the visible region, characterized by two intense bands between 450 and 630 nm and a low reduction potential. In fact, the first reduction process, due to the formation of the radical anion $KuQ^{\bullet-}$ has been observed at -0,3 V *vs*. Ag/AgCl in dichloromethane, which is very low if compared with KuQ analogs, such as Vitamin K_1 or bis-Coenzyme Q_0. A small library of KuQuinone derivatives, differing in the side chain length and functional groups, has been synthesized. Due to their favorable properties, these compounds are good candidates for investigation as photosensitizers on indium-tin oxide (ITO) surface.

Recently, thin films of photoactive molecules on gold[8] and ITO[9] surfaces have attracted much attention as light-harvesting systems in artificial photosynthetic devices.

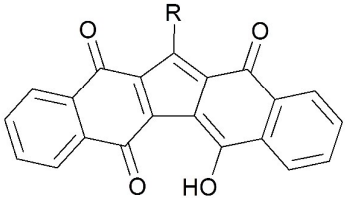

Scheme 1. General structure of KuQuinones.

Dipartimento di Scienze e Tecnologie Chimiche, Università di Roma Tor Vergata, Via della Ricerca Scientifica, 00133, Rome, Italy.
e-mail: galloni@scienze.uniroma2.it, emanuela.gatto@uniroma2.it
Electronic Supplementary Information (ESI) available: [details of any supplementary information available should be included here]. See DOI: 10.1039/x0xx00000x

In this regard, ITO surfaces have been widely used as supports for sensitive materials in photoelectrochemical devices due to their optical transparence and high electrical conductivity[10,11]. Moreover, ITO surfaces are often preferred to gold electrodes because ITO semiconductors usually do not promote excited state quenching of the adsorbed chromophore, resulting more efficient than gold electrodes[9a,12].

In this work, ITO electrodes have been functionalized with substituted KuQuinones by Langmuir-Blodgett technique. Photocurrent generation measurements have been performed using ITO-functionalized surfaces as working electrodes, and the efficiencies of the proposed cells have been evaluated through estimations of the Incident Photon to Current Efficiency values (IPCE %) and internal quantum efficiency (Φ %).

Results and discussion

KuQuinones mono- and multilayers on ITO

The molecular structures of the two KuQuinones used in this work are reported in Scheme 2.

ITO functionalization has been carried out by Langmuir-Blodgett (LB) technique. Amphiphilic KuQ$(CH_2)_9$OH, 1-(9-hydroxynonyl)KuQuinone, is the best candidate for LB deposition, in which electrostatic interactions between hydrophobic 'tails' and hydrophilic 'heads' with an hydrophobic or hydrophilic substrate respectively, are the driving force for the mono- and multilayer growth. Nevertheless, in the present study the deposition of a less polar molecule, such as KuQCH_3, 1-methylKuQuinone, has been also carried out.

Mono- and multilayers deposited on ITO, of both KuQuinones derivatives (Figures. 1-2) are characterized by a broad and intense absorption spectrum in the visible region, between 350 and 630 nm. However, UV-vis spectra of the quinoid compounds on ITO are somewhat different from the spectra in solution[7], since bands between 500 and 600 nm are inverted in relative intensities, broader and slightly red shifted (see Supp. Info).

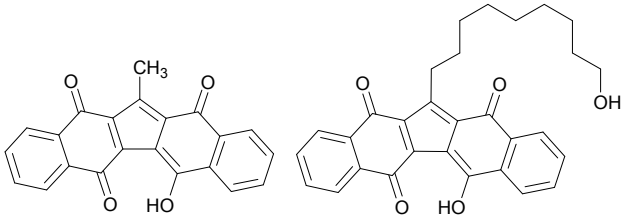

Scheme 2. Chemical structure of 1-methylKuQuinone (left) and 1-(9-hydroxynonyl)KuQuinone (right).

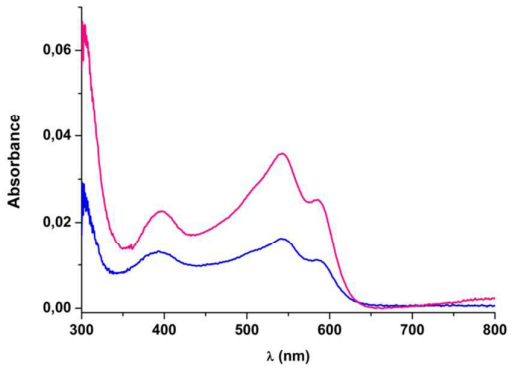

Figure 1. Absorption spectrum of ITO/KuQCH_3: monolayer (blue line); three layers (magenta line).

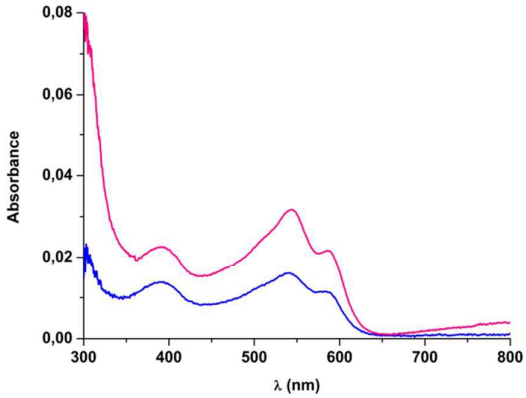

Figure 2. Absorption spectrum of ITO/KuQ$(CH_2)_9$OH: monolayer (blue line); three layers (magenta line).

Differences in the shape of the absorption spectra on ITO surface and in solution likely indicate the simultaneous presence of different species on the surface. As a matter of fact, due to the unusual acidity of the enol proton, the -OH group can be easily deprotonated and the acid-base reaction is strongly influenced by the solvent properties (Scheme 3). In this regard, the predominance of the enol or the enolate form depends on the environment (solvent or surface properties) and it implies differences in terms of spectroscopic behavior. Equilibria between KuQuinones derivatives are discussed elsewhere[13].

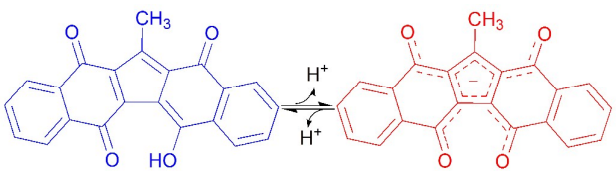

Scheme 3. Acid-base equilibrium of 1-methylKuQuinone

Furthermore, broader and red-shifted spectra on surface are often caused by aggregation phenomena in the adsorbed film[8h,8i,9d,9e]; as to KuQuinone derivatives, aggregation effect could be favored by their planar, pentacyclic and fully conjugated structure.

The absorbed amount of $KuQCH_3$ and $KuQ(CH_2)_9OH$ on ITO was calculated by the absorption spectra of the corresponding films[14]. In particular, considering the co-presence on ITO surface of the KuQuinone, together with the negatively charged enolate, surface coverage values (Γ) have been calculated by equation 1 taking into account both contributions, using molar extinction coefficient in dichloromethane and in basic solution (Supp. Info) and considering a two-dimensional film.

$$\Gamma\left(\frac{\text{molecules}}{\text{cm}^2}\right) = \frac{\text{Absorbance}}{\varepsilon\ (\text{M}^{-1}\cdot\text{cm}^{-1})} \qquad (1)$$

The calculated values were compared with those obtained by the Langmuir-Blodgett apparatus, using the mean area occupied by a single molecule at the deposition pressure used (which is detected by the instrument) and a transfer ratio of approximately 1 for each layer. Results are shown in Table 1.

As it can be seen, reported values for the three layers films are in very good agreement, whilst values calculated for monolayers show small differences. In particular Γ_{LB} are slightly underestimated.

The single molecule occupied mean area at the deposition pressure, determined by the Langmuir-Blodgett instrument, was (13±1) $Å^2$ for $KuQCH_3$ and (22±2) $Å^2$ for $KuQ(CH_2)_9OH$. These so different values can be used to have an idea of the diverse orientation of the two molecules on the ITO surface, taking into account their size, calculated with DFT in vacuum using hybrid functional B3LYP and 6-31G+dp basis set[15]. From such evaluations, it was possible to propose a model that may represent the different spatial arrangement of the molecules on the ITO surface. As to $KuQCH_3$, due to the lack of the hydroxyl group bound to the alkyl side chain, a more disordered film is obtained, where molecules are mainly vertically arranged (the calculated area per molecule the area obtained as vertical projection of the molecule on the surface is (12±1) $Å^2$).

Table 1. Surface coverage calculated by LB (Γ_{LB}) and from absorbance (Γ_{Abs})

LB film	$\Gamma_{LB}\left(\frac{\text{molecules}}{\text{cm}^2}\right)$	$\Gamma_{Abs}\left(\frac{\text{molecules}}{\text{cm}^2}\right)$
ITO/**$KuQCH_3$** monolayer	(7.9±0.8)x10^{14}	(1.2±0.2)x10^{15}
ITO/**$KuQCH_3$** three layers	(2.4±0.2)x10^{15}	(2.2±0.4)x10^{15}
ITO/**$KuQ(CH_2)_9OH$** monolayer	(4.5±0.3)x10^{14}	(7.9±0.9)x10^{14}
ITO/**$KuQ(CH_2)_9OH$** three layers	(1.4±0.1)x10^{15}	(1.3±0.2)x10^{15}

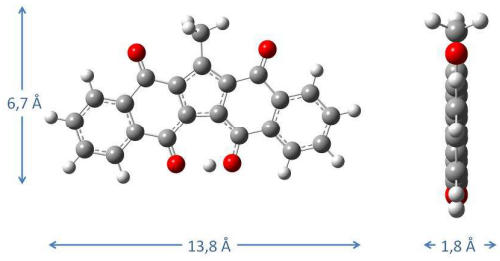

Scheme 4. Optimized structure of $KuQCH_3$, front and side view.

Instead, in the $KuQ(CH_2)_9OH$ film, according to Langmuir-Blodgett principles, terminal hydroxyl group, bonded to the 9-carbon atoms alkyl chain, may interact with the ITO hydrophilic surface, giving rise to the formation of a stable, well packed and ordered film.

In confirmation of that, in this film, the area obtained as horizontal projection of the optimized molecule on the surface is in very good agreement to that recorded by LB instrument. A schematic representation of the proposed spatial arrangements for these molecules on ITO surface is reported in Scheme 5.

Cyclic voltammetry measurements of the ITO modified electrode have been performed in 0.1 M Na_2SO_4 aqueous solution, under nitrogen, with a scan rate of 500 mV/s. The voltammogram of ITO/$KuQCH_3$ electrode showed a broad peak (E½=-0.45 V), probably due to the formation of the radical anion $KuQCH_3^{\bullet-}$ (Figure 3).

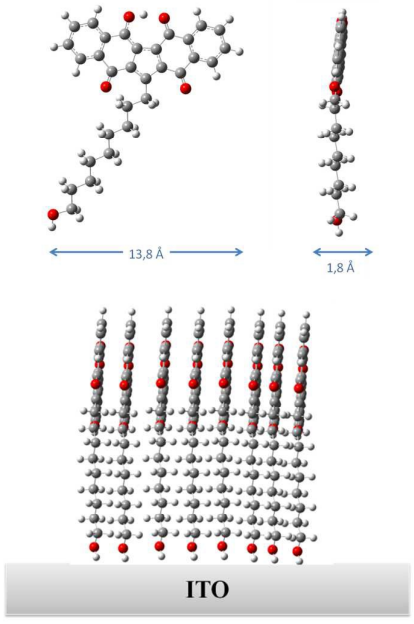

Scheme 5. Optimized structure of $KuQ(CH_2)_9OH$ (front and side view, on the top) and its arrangement on ITO (on the bottom).

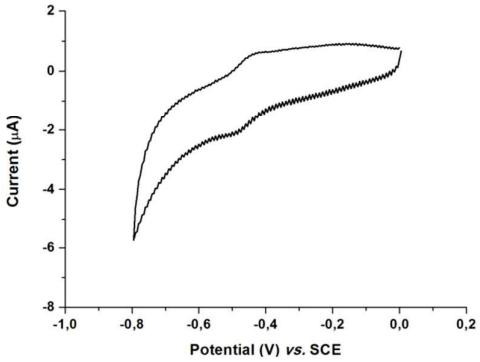

Figure 3. Cyclic Voltammetry of the ITO/KuQCH$_3$ monolayer in H_2O/0.1 M Na_2SO_4 *vs.* SCE; scan rate 500 mV·s^{-1}.

The broadness of the signal likely confirms the hypothesis that the monolayer is not entirely homogeneous. Probably, molecules differently disposed on the surface are affected by different interactions with the chemical environment, leading to a less resolved signal.

With 1-(9-hydroxynonyl)KuQuinone monolayer on ITO, a slightly lower reduction potential (E½=-0.53 V) with respect to that of ITO/KuQCH$_3$ electrode has been detected, possibly because a different organization of the film on the surface (Figure 4). Indeed a reversible one-electron process has been detected, characterized by a well defined peak.

ITO/KuQCH$_3$ photocurrent measurements

Photoelectrochemical measurements were performed in aqueous solution of 0.1 M Na_2SO_4 as supporting electrolyte and 50 mM triethanolamine (TEOA) as electron donor species. The cell was composed by the functionalized ITO/KuQCH$_3$ as working electrode, a platinum counter electrode and an Ag/AgCl (sat. KCl) reference electrode. Irradiation of the ITO/KuQCH$_3$ electrode at different wavelengths resulted in the generation of anodic photocurrent, in which electrons move from the electrolyte to the ITO surface.

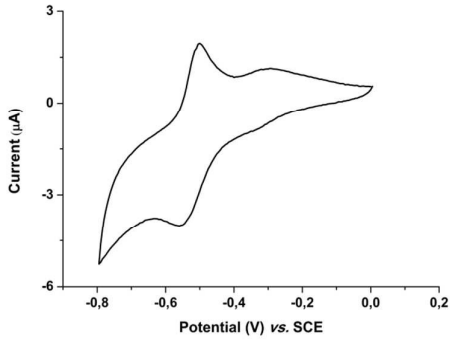

Figure 4. Cyclic Voltammetry of the ITO/KuQ$(CH_2)_9$OH monolayer in H_2O/0.1 M Na_2SO_4 *vs.* SCE; scan rate 100 mV·s^{-1}.

After switching off the illumination, photocurrent immediately dropped down (Figure 5). Increasing the bias potential to the ITO electrode from -0.2 to +0.3 V *vs.* Ag/AgCl, as shown in Figure 6, leads to a strong improvement of the photocurrent signal, reaching the maximum value of 200 nA/cm^2 in the region under 400 nm.

The action spectrum was in good agreement with the absorption spectrum of the modified electrode but it showed an unexpected strong enhancement of the signal in the region between 350 and 400 nm. However, the good relationship between action and absorption spectra of the system indicates that the 1-methylKuQuinone unit acted as a photoactive centre for photocurrent generation. The proposed mechanism of the anodic photocurrent is reported in Figure 7.

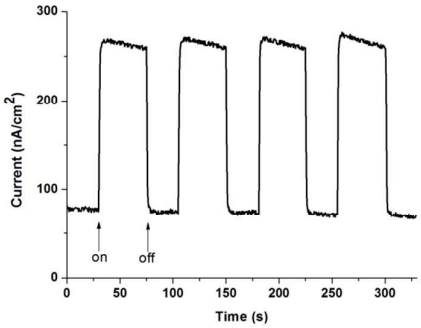

Figure 5. Photoelectrochemical response of ITO/KuQCH$_3$ electrode in H_2O/0.1 M Na_2SO_4/50 mM TEOA, at 0.3 V *vs.* Ag/AgCl, upon irradiation at different wavelengths (from 380 nm to 350 nm every 10 nm) at room temperature; 45 seconds of irradiation were alternated with 30 seconds of dark.

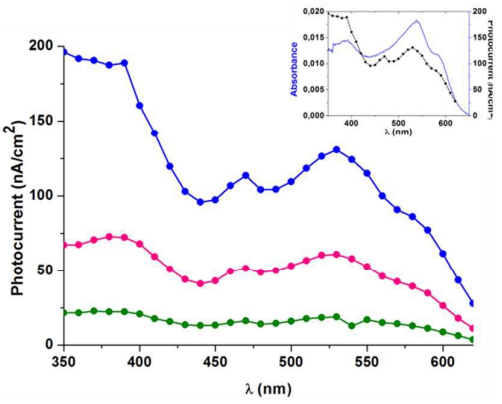

Figure 6. Action spectrum of ITO/KuQCH$_3$ in H_2O/0.1 M Na_2SO_4 /50 mM TEOA. Applied potential: -0.2 V (green line), 0.0 V (pink line), +0.3 V (blue line), *vs.* Ag/AgCl. Inset: Photocurrent action spectrum of ITO/KuQCH$_3$ electrode (blue line) compared to the monolayer absorption spectrum (black line). Applied potential +0.3 V *vs.* Ag/AgCl in H_2O/0.1 M Na_2SO_4 /50 mM TEOA.

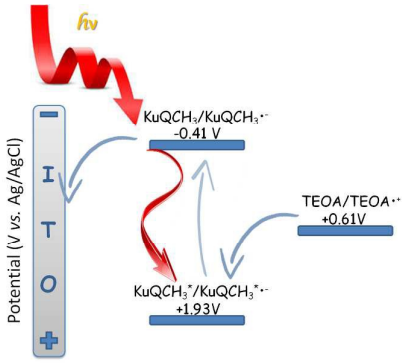

Figure 7. Proposed mechanism for the anodic photocurrent generation in presence of TEOA[16].

Upon irradiation of the functionalized electrode at different wavelengths, 1-methylKuQuinone switches to the excited state, becoming a strong oxidant, which takes an electron from the TEOA in solution. Afterwards, the radical anion formed, $KuQCH_3^{\bullet-}$, is able to give one electron to the conduction band of the ITO surface, closing the circuit.

To confirm the fundamental role of the electron donor species in the cell to close the circuit, photocurrent generation experiments have been performed in the absence of TEOA, obtaining negligible signals under the same conditions (results not shown). Furthermore, experiments have been performed also under nitrogen atmosphere to exclude oxygen from the electrolyte solution, since it might compete with KuQuinone as electron acceptor species, decreasing the efficiency of the cell. Signals comparable to those obtained in the presence of oxygen were observed, leading to the conclusion that oxygen does not significantly affect the anodic photocurrent generation process.

The absorption spectrum of the ITO/$KuQCH_3$ recorded after the photocurrent experiment appeared quite different from the initial spectrum of the monolayer, showing a significant enhancement of the absorption band around 390 nm together with a lower absorption in the range between 500 and 600 nm. Actually, the final absorption spectrum is in good agreement with the reported action spectrum (Figure 8).

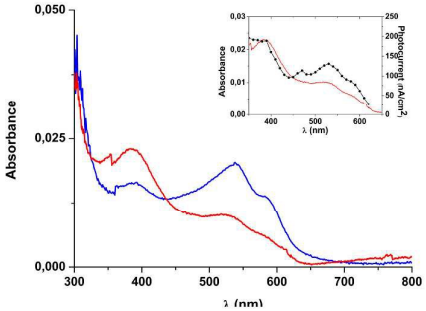

Figure 8. Absorption spectrum of the ITO/$KuQCH_3$ monolayer before (blue line) and after photocurrent experiment in H_2O/0.1 M Na_2SO_4 /50 mM TEOA (red line). Inset: Photocurrent action spectrum of ITO/$KuQCH_3$ electrode (black line) compared to the monolayer absorption spectrum (red line) recorded after the experiment.

In this regard, due to the basic solution in which photocurrent measurements were carried out, the deprotonation of the enol group by the triethanolamine in solution is expected, leading to the formation of the enolate species (Scheme 3), characterized by a broad absorption band below 400 nm in the UV-vis spectrum[13]. Furthermore, because of the higher solubility of the negatively charged quinone moiety in water, a partial detachment of the monolayer from the ITO surface could be also possible.

To support the above assumptions, photocurrent generation experiments have been performed using ascorbic acid (AsA) as electron donor species, overcoming the deprotonation phenomenon by the presence of an acid component in the electrolyte solution. In agreement with our hypothesis, the absorption spectrum after the measurement was comparable to that recorded before (Figure 9), but the efficiency of the latter cell was lower than that of the cell containing TEOA as electron donor: no more than 50 nA/cm^2 have been detected at 0.0 V (a higher applied potential would cause the AsA discharge at the electrode).

On the other hand, photoelectrochemical experiments carried out using ITO functionalized with three layers of $KuQCH_3$ under optimized conditions (H_2O/0.1 M Na_2SO_4 /50 mM TEOA) showed an improvement of the generated photocurrent (Figure 10).

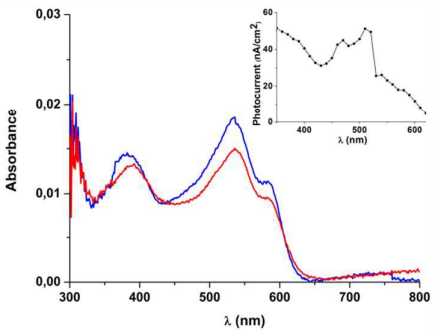

Figure 9. Absorption spectrum of ITO/$KuQCH_3$ before (blu line) and after (red line) photocurrent generation measurement in H_2O/0,1 M Na_2SO_4 /50 mM AsA. Inset: Photocurrent action spectrum of ITO/$KuQCH_3$ electrode in H_2O/0,1 M Na_2SO_4 /50 mM AsA. Applied potential: 0,0 V *vs.* Ag/AgCl.

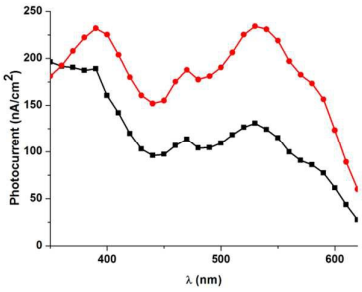

Figure 10. Action spectrum of ITO/$KuQCH_3$ three layers (red line) and monolayer (black line) in H_2O/0.1 M Na_2SO_4 /50 mM TEOA at +0.3 V *vs.* Ag/AgCl.

In particular, although an higher absorbance has been recorded in the entire UV-Vis region, the largest enhancement of photocurrent signal has been detected in the range between 450 and 600 nm.

ITO/KuQ$(CH_2)_9$OH photocurrent measurements

In order to improve the device performance, we used the more stable and spatially ordered monolayer obtained with 1-(9-hydroxynonyl)KuQuinone; therefore, photoelectrochemical performances of the corresponding Langmuir-Blodgett film were evaluated. Measurements have been performed under the same experimental conditions optimized for the ITO/KuQCH_3 electrode. A stable anodic photocurrent signal has been detected irradiating the electrode at +0.3 V applied potential *vs*. Ag/AgCl in 0.1 M Na_2SO_4 aqueous solution containing 50 mM TEOA as electron donor. Interruption of the illumination instantly caused the loss the photocurrent signal (Figure 11).

The photocurrent increases with increasing positive bias to the ITO electrode from -0.2 to +0.3 V *vs*. Ag/AgCl, as shown in Figure 12, giving values almost two times higher than the KuQCH_3 monolayer and reaching the maximum value of 380 nA/cm^2 at 530 nm and +0.3 V.

The action spectra profiles entirely match the absorption spectrum of the modified electrode showing the highest performances in the range between 450 and 600 nm, where the monolayer exhibits its highest absorption.

The good relationship between action and absorption spectra confirms that the quinoid compound acts as sensitizer in the photoelectrochemical device.

The mechanism for the photocurrent generation hypothesized for the ITO/KuQCH_3 functionalized electrode has been confirmed also for this latter film (Figure 13).

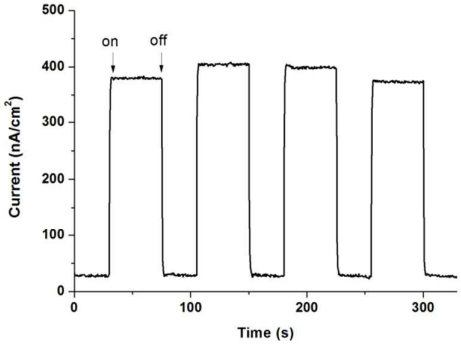

Figure 11. Photoelectrochemical response of ITO/KuQ$(CH_2)_9$OH electrode in H_2O/0.1 M Na_2SO_4 /50 mM TEOA, at 0.3 V vs. Ag/AgCl upon irradiation at different wavelengths (from 520 nm to 550 nm every 10 nm) at room temperature; 45 seconds of irradiation were alternated with 30 seconds of dark.

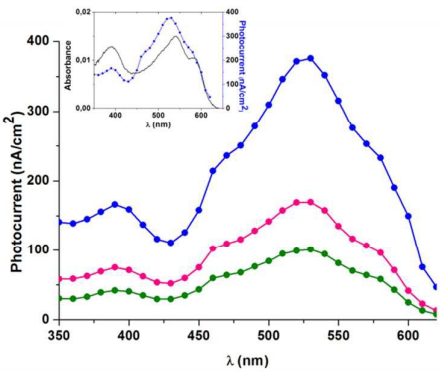

Figure 12. Action spectrum of ITO/KuQ$(CH_2)_9$OH in H_2O/0.1 M Na_2SO_4 / 50 mM TEOA. Applied potential: -0.2 V (green line), 0.0 V (pink line), +0.3 V (blue line), *vs.* Ag/AgCl. Inset: Photocurrent action spectrum of ITO/KuQ$(CH_2)_9$OH electrode (blu line) compared to the monolayer absorption spectrum (black line). Applied potential +0.3 V *vs.* Ag/AgCl in H_2O/0.1 M Na_2SO_4 /50 mM TEOA.

A further strong improvement of the system has been obtained working with a three layers film on the ITO surface (Figure 14). In fact, although the multilayer absorbance was just two times higher than that of the single monolayer, the generated photocurrent was more than quadruplicated, reaching a maximum value of 1.65 μA/cm^2 at 530 nm.

As a result, electron transfer process generated with the amphiphilic KuQuinone derivative resulted more efficient than that obtained with the 1-methylKuQuinone. As a matter of fact, Langmuir-Blodgett technique allows to obtain homogeneous and ordered films of amphiphilic molecules, such as KuQ$(CH_2)_9$OH on a surface, which produced higher photoelectrochemical performances with respect to mono- and multilayers of less polar molecules.

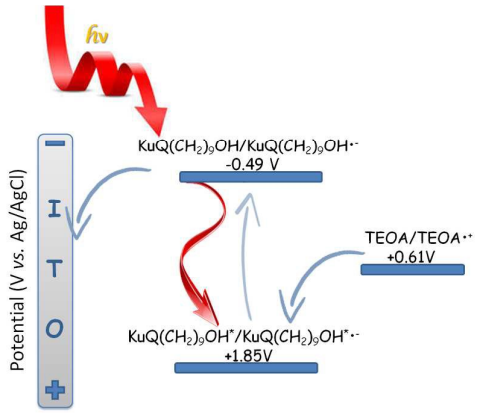

Figure 13. Proposed mechanism for the anodic photocurrent generation in presence of TEOA[16].

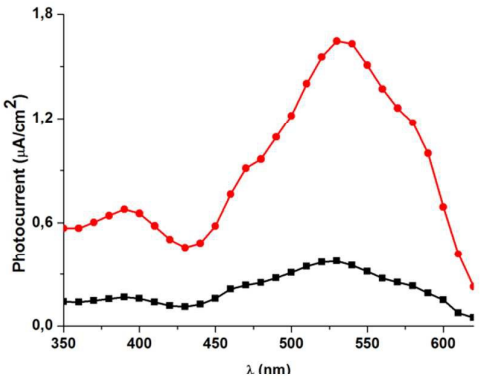

Figure 14. Action spectrum of ITO/KuQ$(CH_2)_9$OH three layers (red line) and monolayer (black line) in H_2O/0.1 M Na_2SO_4 /50 mM TEOA at +0.3 V *vs.* Ag/AgCl.

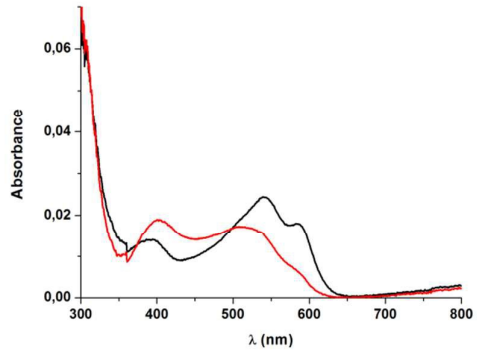

Figure 15. Absorption spectrum of the ITO/KuQ$(CH_2)_9$OH monolayer before (black line) and after photocurrent experiment in H_2O/0.1 M Na_2SO_4 /50 mM TEOA (red line).

The absorption spectrum of the multilayer recorded after the photocurrent generation measurement was affected by the deprotonation effect previously suggested for the KuQCH_3 film (Fig. 15).

Incident Photon to Current Efficiency values (IPCE %) and internal quantum efficiency (Φ %) of the photocurrent generation were calculated at the applied bias potential and excitation wavelength in which the considered system shows the highest photocurrent value. The results are summarized in Table 2.

Table 2. IPCE (%) and Φ (%) values for each functionalized electrode[17,18].

Film	IPCE (%)	Φ (%)
ITO/**KuQCH_3**[a] monolayer	0.02	0.76
ITO/**KuQCH_3**[b] three layers	0.02	0.27
ITO/**KuQ$(CH_2)_9$OH**[b] monolayer	0.03	0.94
ITO/**KuQ$(CH_2)_9$OH**[b] three layers	0.13	2.30

IPCE (%) and Φ (%) values are referred to the H_2O/0.1 M Na_2SO_4 /50 mM TEOA electrolyte solution and they have been calculated at 0.3 V, at the wavelength where the system shows the highest photocurrent value: (a)390 nm and (b)530 nm.

An efficient photoinduced electron transfer has been observed for both, mono- and multilayers of KuQuinones derivatives on ITO. In particular, higher efficiencies have been obtained for the ITO/KuQ$(CH_2)_9$OH in which amphiphilic molecules give rise to a more ordered film than the KuQCH_3 functionalized electrode, which probably implies a well directed electron transfer process.

Concerning the best efficient functionalized electrode, photocurrent measurements have been performed in triplicate; experiments have been carried out with a good reproducibility (the estimated relative error was less than 15%).

Experimental

Instrumentation

Langmuir-Blodgett films have been prepared by using KSV (Helsinki, Finland) LB minitrough equipped with teflon barriers and controlled by the KSV Win LB software. A Wilhelmy balance was used as a surface pressure sensor.

UV–visible absorption spectra were recorded on a Shimadzu 2450 spectrometer equipped with the UV Probe 2.34 program.

Electrochemical experiments were performed with a Palmsens potentiostat. A standard calomel electrode (SCE) was used as the reference electrode, a platinum wire as the auxiliary electrode and the functionalized ITO electrode as the working electrode.

Photocurrent measurements were carried out by using a PG-310 potentiostat (HEKA Elektronik, Lambrecht, Germany) at room temperature. A standard three-electrode configuration was used with ITO modified electrodes as working electrodes and a platinum wire as the auxiliary electrode. The reference electrode was Ag/AgCl. Electrodes were irradiated with a Xe lamp (150 W) equipped with a monochromator. The intensity of the incident light was evaluated with a Vector H410 Power Meter (Scientech, USA).

Materials

All commercial reagents and solvents were used as received, without further purification. 1-MethylKuQuinone (KuQCH_3) and 1-(9-hydroxynonyl)KuQuinone (KuQ$(CH_2)_9$OH) have been synthesized according to a previously reported procedure[7].

ITO electrodes (thickness of ITO coating on transparent glass slides 1200-1600 Å) were commercially available from Aldrich.

Mono- and multilayers preparation

Prior to use, ITO surface was washed in a 1:1 v/v double distilled water/acetone mixture and sonicated for 5 minutes. Afterwards, it was dried under nitrogen and sonicated again, first in 2-propanol and then in dichloromethane.

Mono- and multilayers of KuQuinones have been prepared by Langmuir-Blodgett (LB) technique, at 25°C, on Milli-Q water subphase. 100 µl of 0.2 mg/ml solution of 1-methylKuQuinone or 1-(9-hydroxynonyl)KuQuinone dissolved in chloroform were spread over the subphase. The solvent was allowed to evaporate for 40 minutes. Monolayers were prepared by

emersion of the ITO surface at the rate of 3.6 mm/min and at a surface tension of 30 mN/m (surface pressure values chosen according to isothermal curve plotted for each compound [see Supp info]). Multilayers have been prepared in the same conditions by a series of consecutive emersions and immersions of the ITO electrode. Each single layer was deposited on ITO surface to give a transfer ratio of approximately 1.

Calculation

Computational calculations were performed using Gaussian 09 rev. A.02.[15] Geometry optimizations were performed using hybrid B3LYP functional and 6-31G+(d,p) basis set.

Photocurrent generation measurements

Photocurrent measurements using KuQuinones mono- and multilayers as sensitizers on ITO surface were carried out in a 0.1 M Na_2SO_4 solution containing an electron donor species. A standard three-electrode system was used, with the modified ITO as working electrode, a platinum counter electrode, and Ag/AgCl as reference. The measurements were performed with a certain bias potential and keeping the light on for 45 seconds and then switching it off for 30 seconds. The current measured in the dark was subtracted from the photocurrent generated upon irradiation of the system.

Conclusions

The novel compounds KuQs have been tested as photosensitizers on ITO surface. Usually, quinones are involved in photoinduced electron transfer processes acting as final electron acceptor molecules. Nevertheless, in this work, the polycyclic KuQuinones have been tested also as photosensitizers on ITO electrodes, taking advantage from their broad absorption spectrum in the visible region. This feature, together with their favourable reduction potential, makes them promising dyes and electron acceptor molecules at the same time.

Langmuir-Blodgett deposition resulted as an efficient method to easily obtain homogeneous mono- and multilayers on the ITO-electrode using both, low-polar or amphiphilic KuQuinones derivatives. Promising results in terms of photocurrent generation have been obtained, although efficiencies are affected by the low absorbance of the photoactive material due to the lower surface area of ITO electrode respect to nanoporous surfaces. In particular LB films with the amphiphilic 1-(9-hydroxynonyl)KuQuinone gave the best results in terms of IPCE and Φ, making KuQs good candidates for DSSC.

Acknowledgements

The authors thank PRIN 2010-2011 project 2010M738P for financial support. Dr. Sara Lentini is acknowledged for synthetic assistance and Francesca Valentini for preliminary photocurrent experiments.

Notes and references

1 See as examples: a) I. Agalidis, E. Rivas and F. Reiss-Husson, *Photosynth. Res*., 1990, **23**, 249; b) X. Hu, A. Damjanović, T. Ritz and K. Schulten, *Proc. Natl. Acad. Sci. USA*, 1998, **95**, 5935; c) A. Guskov, J. Kern, A. Gabdulkhakov, M. Broser, A. Zouni and W. Saenger, *Nat. Struct. Bio*., 2009, **16**, 334; d) F. Müh, C. Glöckner, J. Hellmich and A. Zouni, *Biochim. Biophys. Acta*, 2012, **1817**, 44; e) A. G. Gabdulkhakov and M. V. Dontsova, *Biochemistry (Moscow)*, 2013, **78**, 1524; f) K. Saito, A. W. Rutherford and H. Ishikita, *Proc. Natl. Acad. Sci. USA*, 2013, **110**, 954; g) Shikanai, *Curr. Opin. Biotech*., 2014, **26**, 25.

2 See as examples: a) R. Baradaran, J. M. Berrisford, G. S. Minhas and L. A. Sazanov, *Nature*, 2013, **494**, 443; b) P. Hellwig, *Biochim. Biophys. Acta*, 2015, **1847**, 126; c) M. Sarewicz and A. Osyczka, *Physiol Rev.,* 2015*,* **95**, 219.

3 See as examples: a) S. Nawar, B. Huskinson and M. Aziz, *Mater. Res. Soc. Symp. Proc*., 2013, 1491; b) S. Er, C. Suh, M. P. Marshak and A. Aspuru-Guzik, *Chem. Sci*., 2015, **6**, 885.

4 M. Kato, T. Cardona, A. W. Rutherford and E. Reisner, *J. Am. Chem. Soc*., 2012, **134**, 8332.

5 See as examples: a) M. R. Wasielewski and M. P. Niemczyk, *J. Am. Chem. Soc*., 1984, **106**, 5043; b) R. Borrelli and W. Domcke, *Chem. Phys. Lett*., 2010, **498**, 230; c) C. A. Wijesinghe, M. Niemi, N. V. Tkachenko, N. K. Subbaiyan, M. E. Zandler, H. Lemmetyinen and F. D'Souza, *J. Porphyrins Phthalocyanines* 2011, **15**, 391; d) M. Kanematsu, P. Naumov, T. Kojima and S. Fukuzumi, *Chem. Eur. J*., 2011, **17**, 12372; e) Y. K. Kang, P. M. Iovine and M. J. Therien, *Coord. Chem. Rev*., 2011, **255**, 804.

6 a) J. Q. Chambers in The Chemistry of Quinoid Compounds. Vol. II, Chapter 12, Eds. S. Patai, Z. Rappoport, John Wiley & Sons Ltd., 1988; b) P. Sarathi Guin, S. Das and P. C. Mandal, *Int. J. Electrochem*., 2011, article id 816201.

7 A. Coletti, S. Lentini, V. Conte, B. Floris, O. Bortolini, F. Sforza, F. Grepioni and P. Galloni, *J. Org. Chem*., 2012, **77**, 6873.

8 See as examples: a) H. Imahori, H. Yamada, S. Ozawa, K. Ushidab and Y. Sakata, *Chem. Commun.*, 1999, 1165; b) M. J. den Hollander, J. G. Magis, P. Fuchsenberger, T. J. Aartsma, M. R. Jones and R. N. Frese, L*angmuir*, 2011, ***27***, 10282; c) A. Vecchi, E. Gatto, B. Floris, V. Conte, M. Venanzi, V. N. Nemykin and P. Galloni, *Chem. Commun*., 2012, **48**, 5145; d) E. Gatto, M. Caruso, C. Toniolo, F. Formaggio, M. Crisma and M. Venanzi, *J. Pept. Sci*., 2011, **17**, 124; e) M. Venanzi, E. Gatto, M. Caruso, A. Porchetta, F. Formaggio and C. Toniolo, *J. Phys. Chem. A,* 2014, **118**, 6674; f) A. Vecchi, N. R. Erickson, J. R. Sabin, B. Floris, V. Conte, M. Venanzi, P. Galloni and V. N. Nemykin, *Chem. Eur. J*., 2015, **21**, 269; g) H. Uji, Y. Yatsunami and S. Kimura, *J. Phys. Chem. C,* 2015, **119**, 8054; h) H. Imahori, H. Norieda, Y. Nishimura, I. Yamazaki, K. Higuchi, N. Kato, T. Motohiro, H. Yamada, K. Tamaki, M. Arimura and Y. Sakata, *J. Phys. Chem. B*, 2000, **104**, 1253; i) H. Imahori, H. Yamada, Y. Nishimura, I. Yamazaki and Y. Sakata, *J. Phys. Chem. B*, 2000, **104**, 2099.

9 See as examples: a) H. Yamada, H. Imahori, Y. Nishimura, I. Yamazaki and S. Fukuzumi, *Chem. Commun*., 2000, 1921; b) H. Yamada, H. Imahori, Y. Nishimura, I. Yamazaki and S. Fukuzumi, *Adv. Mater*., 2002, **14**, 892; c) H. Imahori, M. Kimura, K. Hosomizu, T. Sato, T. K. Ahn, S. K. Kim, D. Kim, Y. Nishimura, I. Yamazaki, Y. Araki, O. Ito, S. Fukuzumi and *Chem. Eur. J*., 2004, **10**, 5111; d) M. Isosomppi, N. V. Tkachenko, A. Efimov, K. Kaunisto, K. Hosomizu, H. Imahori and H. Lemmetyinen, *J. Mater. Chem*., 2005, **15**, 4546; e) N.

Araki, M. Obata, A. Ichimura, Y. Amao, K. Mitsuo, K. Asai and S. Yano, *Electrochim. Acta*, 2005, **51**, 677; f) M. Hyung Lee, J. Won Kim and C. Yeon Lee, *J. Organomet. Chem*., 2014, **761**, 20.

10 N. R. Armstrong, C. Carter, C. Donley, A. Simmonds, P. Lee, M. Brumbach, B. Kippelen, B. Domercq and S. Yoo, *Thin Solid Films*, 2003, **445**, 342.

11 S. Lee, J. H. Noh, S. T. Bae, I. S. Cho, J. Young Kim, H. Shin, J. K. Lee, H. Suk Jung and K. Sun Hong, *J. Phys. Chem. C,* 2009, **113**, 7443.

12 H. Yamada, H. Imahori, Y. Nishimura, I. Yamazaki, T. Kyu Ahn, S. Keun Kim, D. Kim and S. Fukuzumi, *J. Am. Chem. Soc.* 2003, **125**, 9129.

13 PhD thesis in Chemical Sciences, Sara Lentini, **2014** University of Rome Tor Vergata.

14 B. O'Regan and M. Grätzel, *Nature*, 1991, **353**, 737.

15 M.J. Frisch, G.W. Trucks, H.B. Schlegel, G.E. Scuseria, M.A. Robb, J.R. Cheeseman, G. Scalmani, V. Barone, B. Mennucci, G.A. Petersson, H. Nakatsuji, M. Caricato, X. Li, H.P. Hratchian, A.F. Izmaylov, J. Bloino, G. Zheng, J.L. Sonnenberg, M. Hada, M. Ehara, K. Toyota, R. Fukuda, J. Hasegawa, M. Ishida, T. Nakajima, Y. Honda, O. Kitao, H. Nakai, T. Vreven, J.A. Montgomery Jr., J.E. Peralta, F. Ogliaro, M. Bearpark, J.J. Heyd, E. Brothers, K.N. Kudin, V.N. Staroverov, R. Kobayashi, J. Normand, K. Raghavachari, A. Rendell, J.C. Burant, S.S. Iyengar, J. Tomasi, M. Cossi, N. Rega, J.M. Millam, M. Klene, J.E. Knox, J.B. Cross, V. Bakken, C. Adamo, J. Jaramillo, R. Gomperts, R.E. Stratmann, O. Yazyev, A.J. Austin, R. Cammi, C. Pomelli, J.W. Ochterski, R.L. Martin, K. Morokuma, V.G. Zakrzewski, G.A. Voth, P. Salvador, J.J. Dannenberg, S. Dapprich, A.D. Daniels, O. Farkas, J.B. Foresman, J.V. Ortiz, J. Cioslowski, D.J. Fox, Gaussian 09, Revision A.02, Gaussian, Inc., Wallingford CT, 2009.

16 M. Julliard and M. Channon, *Chem. Brit*., 1982, 558. The oxidation potential for the excited state, $E_0(M^*/M^-)$, has been calculated from the equation $E_0(M^*/M^-) = E_0(M/M^-) + E_{0\text{-}0}(M\text{-}M^*) = E_0(M/M^-) + hc/\lambda$, where M is the ground state, M* the lowest excited state, $E_0(M/M^-)$ is the ground state electrochemical redox potential for the couple M/M^- and $E_{0\text{-}0}(M\text{-}M^*)$ is the 0-0 spectroscopic transition energy gap. The first one electron reduction potential has been used as $E_0(M/M^-)$.

17 IPCE is defined as the ratio of the electron injected in the external circuit to the number of incident photons. It can be evaluated through the equation: $IPCE(\%)=100\cdot1240\cdot i\ (W\cdot\lambda)^{-1}$, where i is the photocurrent density ($A\cdot cm^{-2}$), W the incident light intensity (W) and λ the excitation wavelength (nm)[9c].

18 Φ is the quantum yield of photocurrent generation, obtained by the equation: $\Phi(\%)=100\cdot i\cdot e^{-1}\cdot[I(1\text{-}10^{-Abs})]^{-1}$, where $I= W\cdot\lambda\cdot(hc)^{-1}$, i is the photocurrent density, e is the elementary charge, I the numbers of photons per unit area and unit time, λ the wavelength of light irradiation, Abs the absorbance of the adsorbed dye at λ, W the light power irradiated at λ, c the velocity of light and h the Plank constant[9c].

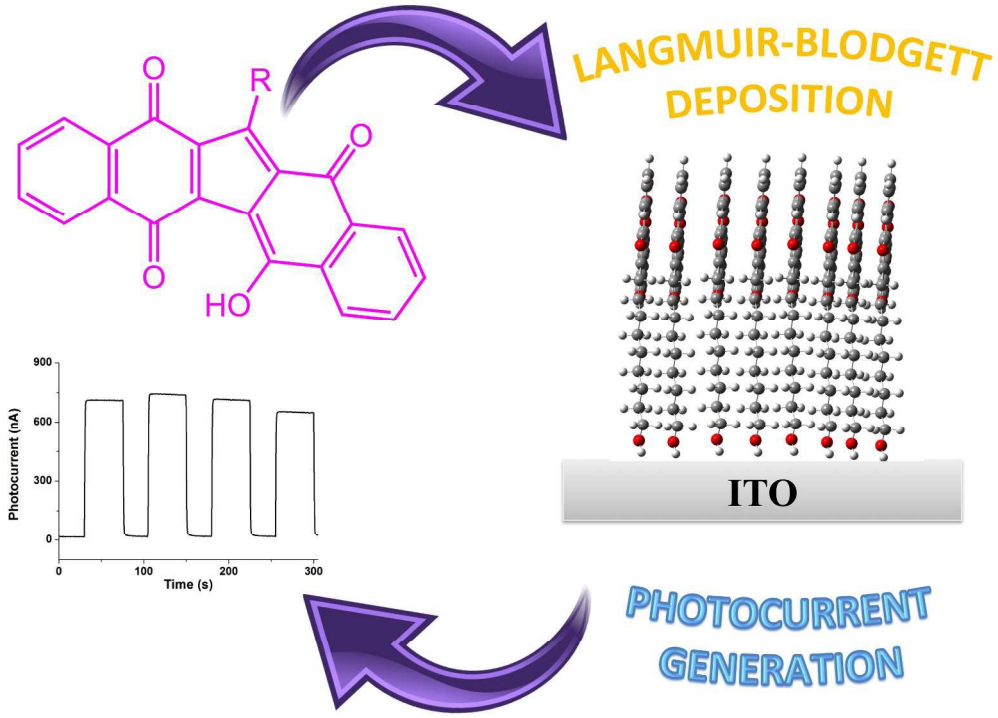

1057x793mm (72 x 72 DPI)